Science Justification

Galaxies form inside Cold Dark Matter (CD) halos[1] that grow by mergers (major, minor, gas-rich, and dry)[2,3,4,5] with other halos and gas accretion[6]. The baryonic physics behind galaxy evolution is aggressively debated and forms the basis of the current areas of research. The formation of the main baryonic components of galaxies (bulges, disks, and bars) is not entirely understood, though it appears that 1) most stellar mass was in place by $z \sim 1$[15] and 2) internal secular evolution[11] dominates the shaping of most galaxies. The frontier lies in understanding the underlying small-scale physics (e.g., star formation (SF), dissipation, feedback[16]), which when combined with gravitational effects from warps, bars, and disks, significantly impacts large scale properties.

VENGA is a nearly complete, ongoing IFU survey of nearby spiral galaxies. The sample contains a range of Hubble types, galaxies with classical bulges and pseudobulges, as well as barred and unbarred objects. Most galaxies have ancillary data from a variety of sources, including *HST*, *Spitzer*, GALEX, CO maps from BIMA SONG[7] and the CARMA CO survey STINGS[8], and archival HI 21 cm maps. The unique role of VENGA is to combine good spatial resolution with excellent spatial and spectral coverage. Consequently, the VENGA data is well-suited to explore the small-scale physics driving the important evolutionary processes. For Trimester 1, we will revisit galaxies having incomplete coverage in the VIRUS-P red and blue spectral setups. We will also extend the high-resolution VIRUS-W survey by gathering more data for galaxies with and without existing VIRUS-W coverage. New VIRUS-W observations complement the existing VIRUS-P data. Below we discuss the project that will benefit most from combining VIRUS-P and VIRUS-W data.

The Assembly, Structure, Morphology, and Kinematics of Bulges in Spirals (Weinzirl, Jogee, Fabricius, Drory, Fisher):

There is abundant evidence that objects photometrically identified as bulges in spiral galaxies are not physically homogeneous. Spiral galaxy bulges can be divided into elliptical-like classical bulges, disk-like pseudobulges, and composite structures[13,28] containing both classical and pseudobulge components. Classical bulges and pseudobulges differ in a variety of characteristics, including structure, morphology, kinematics, stellar populations, and star formation[9,11,13,19,29]. The disparity in the physical properties and scaling relations[13] among the kinds of bulges have implications on the formation mechanisms that shape and assemble not only bulges, but also galaxies as a whole. Within the local Universe, observations suggest an absence of classical bulges such that giant galaxies with bulges resembling relaxed/virialized remnants of major mergers are in the minority[9,11,29].

A complete picture of bulge assembly, and thus galaxy assembly, requires a parallel investigation of multiple bulge properties (structure, star formation history, stellar populations, chemical abundances, and kinematics). Unfortunately, kinematic properties of disk-like bulges remains poorly understood. The reason lies partly in the general unavailability of suitable instrumentation. Tiling long-slit observations, though expensive, has shown a correlation between bulge type and dispersion profile[31]. Still, true 2D kinematic data are necessary to constrain the orbital structure of these objects to confirm the fundamentally different kinematic structure and formation channels. Most existing IFUs that offer suitable spectral resolution typically have high spatial resolution and therefore a field of view too small to cover the bulge regions of local spiral galaxies.

The large field of view and the spectral resolution of VIRUS-W[30] specifically addresses low-dispersion local spiral disks and bulges[29] and complements the lower resolution and broader spectral coverage of the VIRUS-P data with kinematic information. The union of VIRUS-P and VIRUS-W data will in particular enable us to extend the studies of parameter correlations among bulges to include localized kinematic and stellar population parameters. The VIRUS-P data will give a handle on the underlying stellar populations, star formation history, and metallicities, so that we will for the first time be able to probe how these correlate on large scales with kinematic properties such as the local v, σ, h_3 and h_4 momentas (e.g., Figure 1).

Description of Observations & Justification of Exposure Times

VIRUS-P: Our present goal is to view each pointing in Table 1 at the blue (3600-5800 Å) and red (4600-6800 Å) ends of the optical spectrum. Some of these pointings were partially observed in the past but remain unfinished. Acquiring this extra data will complete the red and blue VIRUS-P coverage for 29/30 VENGA targets. Depending on the target (see Table 1), several pointings will be revisited for a total of 14 pointings (5 in the red, 9 in the blue). The 1/3 IFU filling factor requires 3 dithers per pointing to achieve full coverage, translating into 42 effective pointings. The extensive coverage of the bulges, bars, and outer disk (reaching to 0.7 R_{25} in most cases) is only possible thanks to the extremely large 1.7' x 1.7' field of view (FOV) of VIRUS-P[12]. Furthermore, with its fat 4.3" fibers, VIRUS-P is extremely fast for observing extended low surface brightness sources, making it the optimal instrument for conducting this survey. Obtaining this much spatially resolved spectroscopy on this sample in less observing time is beyond the reach of any other instrument at any other telescope.

We will use a low-resolution grating that provides an instrumental resolution of $\sigma_{\rm inst} = 120$ kms^{-1}. The blue setup covers many important features not visible in the existing red VENGA data, like the Balmer break, CaII H+K in absorption, the higher-order Balmer lines (Hγ to Hη, both in absorption and emission), and the [OII] $\lambda\lambda$3726, 3729 Å doublet. The red setup provides additional emission lines like [NII] $\lambda\lambda$6548, 6584 and [SII] $\lambda\lambda$6717, 6731. These lines will be used to construct 2D emission, absorption, and kinematic maps of each galaxy. Synthesis of the red and blue VIRUS-P wavelength coverage with the existing GALEX UV data and *Spitzer* IR data data will be effective at breaking age-metallicity-dust degeneracies in stellar population modeling. Additionally, observing in each of the blue and red setups will boost the S/N for features present in both spectral setups (Hβ, Mg b, Fe, and [OIII]), making the spatial bins smaller in the outer disks of galaxies (e.g., see Figure 2).

Our target S/N (per resolution elements in the continuum) for the spectra is set by our ability to recover central velocities for the stellar component. Monte Carlo simulations show that at S/N= 40 we recover central velocities to ± 2 kms^{-1} from CaII H+K. The exposure time required to reach S/N= 40 is calculated from previous observations of M51a. The average on-source observing time to complete each pointing is ~ 3 hours counting overhead for readout time and sky dithers. Assuming 9 hours of data per night, we can complete $\sim 2.5 - 3$ pointings per night.

VIRUS-W: Being similar to VIRUS-P, the VIRUS-W IFU consists of 267 optical fibers (3.2" in diameter at the 2.7m). The field of view ($1.8' \times 0.9'$ with a 1/3 filling factor) is rectangular and slightly smaller than that of VIRUS-P. The higher spectral resolution mode to be used in VENGA covers 4850-5450Å and has a spectral resolution of 0.78Å FWHM ($\sigma_{\rm inst} \sim 20$km s^{-1}). The most important kinematic stellar absorption features in the VIRUS-W higher resolution spectral coverage are the Mg feature $\lambda\lambda$5167,5172,5183 and the Fe lines $\lambda\lambda$5270,5335,5406. The VIRUS-W observations are more time intensive, and reaching S/N= 30 requires scaling the VIRUS-P exposure times by a factor of ~ 4. Our plan is to obtain coverage of the center pointings in ~ 8 bright galaxies at a rate of 1 galaxy per night. VIRUS-W is bench mounted and therefore not attached to the telescope tube. Identical mechanics to the VIRUS-P IFU head simplifies exchanging the two instruments.

References:
[1]Blumenthal et al. 1984, Natur.311.517B; [2]Navarro & Steinmetz 2002, NewA.7.155S; [3]Eliche-Moral et al. 2006, A&A.457.91E; [4]Hopkins et al. 2009, ApJS.181.135H; [5]van Dokkum 2005, AJ.130.2647V; [6]Dekel et al. 2009, ApJ.703.785D; [7]Helfer et al. 2003, ApJS.145.259H; [8]http://www.astro.umd.edu/bolatto/STING/index.html; [9]Weinzirl et al. 2009, ApJ.696.411W; [10]Yoachim et al. 2010, ApJ.716L.4Y; [11]Kormendy & Kennicutt 2004, ARA&A.42.603K; [12]Hill et al. 2008, ASPC.399.115H; [13]Fisher & Drory 2010, ApJ.716.942F; [14]Bacon et al. 2001, MNRAS.326.23; [15]Dickinson et al. 2003, 2003, ApJ.587.25; [16]Hopkins et al. 2009, ApJ.691.1168; [17]Kennicutt et al. 2003, PASP.115.928; [18]Dong & De Robertis 2006, AJ.131.1236D; [19]Fisher & Drory 2008, AJ.136.773F; [20]Bigiel et al. 2008, AJ.136.2846B; [21]Kennicutt et al. 2007, ApJ.671.333K; [22]Blanc at al. 2008, ApJ.704.842; [23]Hill et al. 2008, ASPC.399.115H; [24]Rokar et al. 2008, ApJ.675.L65; [25]Thilkeret et al. 2005, ApJ.619.L79; [26]Navarro et al. 1997, ApJ.490.493; [27]Kormendy, J. 1993, Proceedings of IAU Symposium 153, 209; [28]Kormendy, J., & Barentine, J. C. 2010, ApJ.715L.176K; [29]Kormendy et al. 2010,ApJ.723.54K; [30]Fabricius et al. 2008, SPIE.7014E.234F; [31]Fabricius et al. 2011, *in prep*; [32]Adams et al. 2010, ApJS.192.5; [33]Blanc et al. 2011, ApJ.736.31B;

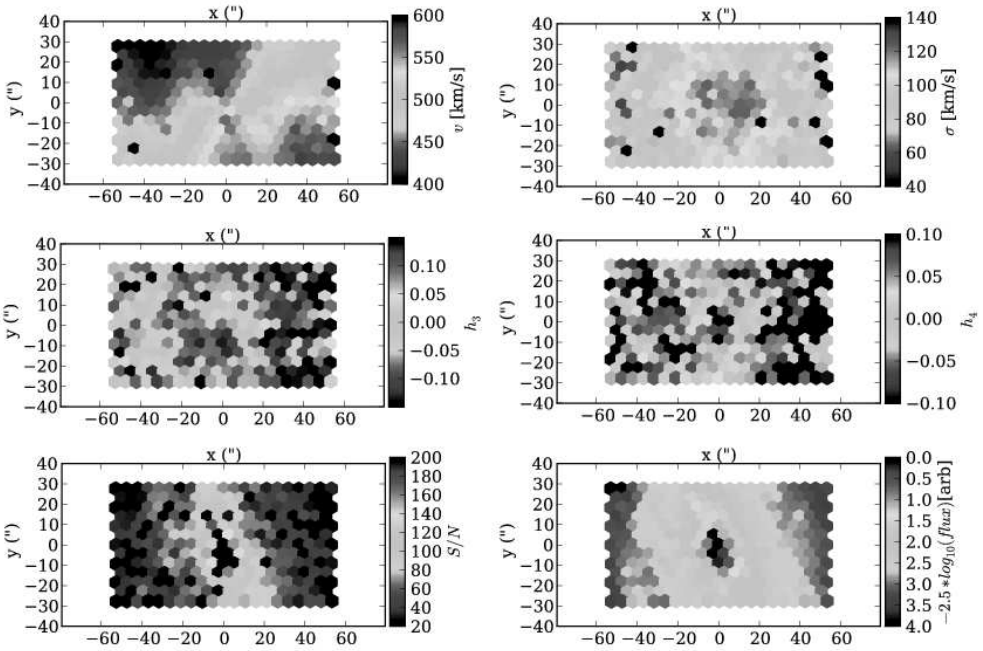

Figure 1 VIRUS-W maps of NGC 2903 showing stellar kinematic properties (v, σ, h_3 and h_4 momentas), S/N, and integrated light. The cumulative exposure time is 3.5 hours, a factor of 3 times longer than the VIRUS-P exposure time. The bottom left panel shows an S/N of ~ 200 was reached in the nucleus while at the edges of the exposure the S/N is $\sim 20 - 30$.

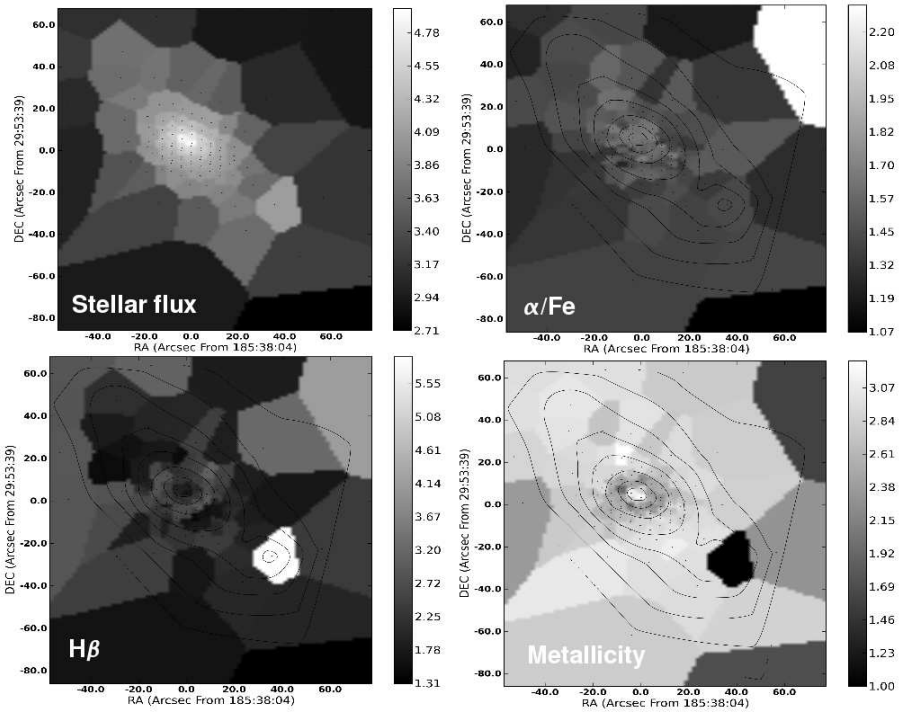

Figure 2 Virus-P maps of NGC 4314. This galaxy features a bar and a nuclear star-forming ring. From upper left to lower right: a) Stellar continuum; b) α/Fe abundance ratio; c) Hβ absorption; d) Metallicity. The upper right and lower plots show contours from the stellar continuum map. All maps are binned to $S/N = 75$. The star-forming ring is visible in panels b and d as a decline in $[\alpha/Fe]$ and metallicity relative to the bulge, and in panel c as an enhancement in Hβ.

Table 1. Trimester 1 VENGA Targets

Object	Equatorial Coord.		Type	D_{25}	N_P[a]	μ_{B25}[b]	B/T	n_{Bulge}	VP Red[f]	VP Blue[f]	Need VW[g]
	α	δ		arcmin		mag arcmin^{-2}					
NGC1042[d]	02:40:24.0	-08:26:02	SAB(rs)cd	4.7x3.6	-	14.47	0.03	0.10	F	F	y
NGC2775[d]	09:07:58.4	+41:42:37	SA(r)ab	4.3x3.3	-	13.76	0.61	4.85	F	F	y
NGC2841[e]	09:22:01.8	+50:58:31	SA(r)b	8.1x3.5	-	13.57	0.17	2.97	F	F	y
NGC2903[e]	09:32:09.7	+21:30:02	SB(s)d	12.6x6.0	-	14.21	0.09	0.42	F	F	y
NGC3227[d]	10:23:31.5	+19:51:48	SAB(s)pec	5.4x3.6	-	14.19	0.10	0.32	F	F	y
NGC3521[c]	11:05:49.0	-00:02:15	SAB(rs)bc	11.0x5.1	1	14.04	0.10	3.20	F	P	y
NGC3949[d]	11:53:41.5	+47:51:35	SA(s)bc	2.9x1.2	-	13.09	0.08	0.64	F	F	y
NGC4013	11:58:31.7	+43:56:48	SAb	5.2x1.0	2	13.86	-	-	F	P	n
NGC4314[d]	12:22:32.2	+29:53:47	SB(rs)a	4.2x3.7	6	14.24	0.26	2.05	P	N	y
NGC4450[d]	12:28:29.4	+17:05:05	SA(s)ab	5.2x3.9	3	14.00	0.17	2.26	P	N	n
NGC4569[e]	12:36:50.1	+13:09:48	SAB(rs)ab	9.5x4.4	1	14.19	0.06	1.90	F	P	n
NGC6946[e]	20:34:52.3	+60:09:14	SAB(rs)cd	11.5x9.8	1	14.58	0.01	1.87	P	F	n

[a]Combined number of red and blue VIRUS-P pointings to be revisited

[b]RC3

[c,d,e]Bulge parameters (B/T, n_{bulge}) from (c) K-band decomposition[18], (d) H-band decomposition[9], (e) V-band decomposition[19]

[f]Observing status: Fully observed (F), Partially observed (P), or Not yet observed (N)

[g]Plan to observe with VIRUS-W: Yes (y), No (n)

Description & Justification of Special Constraints

A combination of dark and gray time is required for the targets in Table 1. Dark time is preferable for observing the lowest surface brightness targets and the outer parts of the disks of most galaxies. Gray time is well suited for the brightest targets and the central parts of most galaxies. Ideally the nights awarded should be ±8 days from new moon.

We request that 15 nights be awarded. Of these, 7 should allocated for the VIRUS-P observations. The VIRUS-P targets will best be observable in the middle-to-end of March. The other 8 nights should be allocated to VIRUS-W.

Results from Previous Observing Time at McDonald

VENGA has been awarded 149 nights in total. At the time of this submission, we have observed 141 nights. (Eight nights were lost due to dome painting and the wildfire.) We lost 43 nights to a combination of bad weather, technical problems, dome painting, and the wildfire, leaving 106 nights of usable data. At this stage we have almost finished the VIRUS-P observations, and after the upcoming Trimester 1, the VIRUS-P data will be complete for 29/30 targets. In the future, we expect to ask for more time on VIRUS-P only if the need arises.

Blanc, Heiderman, Gebhardt and Evans have used the VENGA data to measure the spatially resolved Schmidt law in M51 (NGC 5194). We have used extinction corrected Hα fluxes to construct an SFR map. This map, together with CO J=1-0 maps from BIMA SONG[7] and archival HI 21cm maps, were used to construct the Schmidt law for molecular and atomic hydrogen. The best fit power-law shows a slope of 0.83±0.30, in good agreement with the 0.82±0.19 value obtained by [20], but in large disagreement with the 1.37±0.03 value obtained by [21] for the same galaxy. These two are the only previous studies of the "spatially resolved" Schmidt law, and they both used imaging (GALEX UV and ground based Hα narrow-band respectively, combined with 24μm MIPS) to estimate the SFR. Integral field spectroscopy allows a much cleaner measurement of Hα emission line fluxes than narrow-band imaging, since it is free of the systematics introduced by continuum subtraction, underlying photospheric absorption, and contamination by the [NII] doublet. The Schmidt Law is an important observable to test theories of high mass star formation, and it is widely used as a SFR recipe in cosmological semi-analytical simulations of galaxy formation. A paper showing these results has been recently published in ApJ[22]. This is the first refereed publication associated with VENGA.

Gebhardt, Hill, Hao and Blanc have commissioned and used VIRUS-P to conduct the HETDEX Pilot Survey. We have observed ∼200 arcmin of blank sky in the COSMOS, GOODS-N, MUNICS and XMM-LSS fields, looking for Lyman Alpha Emitting galaxies (LAE) at $2 < z < 4$. Early results of the survey, showing the effectiveness of integral field spectroscopy for detecting high redshift galaxies can be found in [23]. We have a final sample of objects, and have multiple papers in progress. The two main papers ([32], [33]) have been published.

Yoachim has used VIRUS-P to target a sample of face-on disk galaxies to measure stellar population gradients. He has traced the age and metallicity of stellar populations to large radii, where the surface brightness profile truncates and is no longer described by a single exponential. He is in the process of testing two primary models proposed for creating the observed breaks. In the first, a star formation threshold creates a sharp truncation radius and the outer regions of the disk are populated by stars that have gravitationally scattered from the interior[24]. In the second, star formation in the outer regions of galaxies simply becomes inefficient and must rely on non-gravitational cloud collapse mechanisms[25]. In addition, Yoachim finds from spatially resolved spectra of NGC 6155 that stellar age increases significantly beyond the galaxy stellar break radius[10].

Gebhardt has used VIRUS-P to study the properties of DM halos around elliptical galaxies, by measuring the kinematics of integrated stellar light at large radii (few R_e). First results show that DM is necessary to explain the velocity dispersions observed at these radii, and further modeling will put constrains on the shape of DM halo profiles. This work will serve as a test for DM halo profiles predicted by ΛCDM theory[26].